Hindawi Publishing Corporation
International Journal of Photoenergy
Volume 2015, Article ID 483147, 8 pages
http://dx.doi.org/10.1155/2015/483147

Research Article

Improving Performance of CIGS Solar Cells by Annealing ITO Thin Films Electrodes

Chuan Lung Chuang,[1] Ming Wei Chang,[1] Nien Po Chen,[1] Chung Chiang Pan,[1] and Chung Ping Liu[1,2]

[1]*Department of Photonics Engineering, Yuan Ze University, 135 Yuan-Tung Road, Chungli 320, Taiwan*
[2]*Department of Physics, Fu Jen Catholic University, 510 Zhongzheng Road, Xinzhuang District, New Taipei 242, Taiwan*

Correspondence should be addressed to Chuan Lung Chuang; s979001@mail.yzu.edu.tw
and Chung Ping Liu; eecpliu@saturn.yzu.edu.tw

Received 19 July 2015; Revised 11 October 2015; Accepted 22 October 2015

Academic Editor: Elias Stathatos

Indium tin oxide (ITO) thin films were grown on glass substrates by direct current (DC) reactive magnetron sputtering at room temperature. Annealing at the optimal temperature can considerably improve the composition, structure, optical properties, and electrical properties of the ITO film. An ITO sample with a favorable crystalline structure was obtained by annealing in fixed oxygen/argon ratio of 0.03 at 400°C for 30 min. The carrier concentration, mobility, resistivity, band gap, transmission in the visible-light region, and transmission in the near-IR regions of the ITO sample were $-1.6E + 20$ cm^{-3}, $2.7E + 01$ cm^2/Vs, $1.4E - 03$ Ohm-cm, 3.2 eV, 89.1%, and 94.7%, respectively. Thus, annealing improved the average transmissions (400–1200 nm) of the ITO film by 16.36%. Moreover, annealing a copper-indium-gallium-diselenide (CIGS) solar cell at 400°C for 30 min in air improved its efficiency by 18.75%. The characteristics of annealing ITO films importantly affect the structural, morphological, electrical, and optical properties of ITO films that are used in solar cells.

1. Introduction

Indium tin oxide (ITO) film has highly favorable properties, such as low resistivity (~10^{-4} Ohm-cm), high optical transmittance for visible light, and high near-infrared reflectance, making it effective as an n-type window layer, particularly in solar cells [1, 2]. Chalcopyrite compounds of copper-indium-gallium-diselenide (CIGS) and related alloys are among the most promising materials for photovoltaic applications [3]. The highest conversion efficiency of CIGS solar cells that has so far been obtained is 21.7% [4].

ITO thin films can be prepared using many techniques, including e-beam evaporation [5, 6], plasma-enhanced metal organic chemical vapor deposition [7], pulsed laser deposition [8], dip coating [9], ion beam sputtering [10], magnetron sputtering [11], and thermal evaporation [12]. Among these for forming ITO thin films, magnetron sputtering has the advantage of being able to form films of high quality at room temperature [13–16], which can be used to coat large areas [17, 18]. Postdeposition annealing at temperatures of more than 200°C has been shown to be effective in improving the grain growth and crystallinity of ITO thin films [19–21].

In this work, ITO thin films were grown on glass substrates by direct current (DC) magnetron reactive sputtering at room temperature. Annealing at the optimal temperature can greatly improve the composition and structural, optical, and electrical properties of the ITO film. ITO samples with a thickness of ~300 nm were deposited on glass. Some of the ITO film samples were deposited at room temperature using a fixed oxygen/argon ratio of 0.03 before being annealed at various temperatures (as-grown/100°C/200°C/300°C/400°C) for 30 min in air.

2. Experimental Method

ITO thin films were deposited by DC reactive magnetron sputtering from an oxide ceramic target of 90 wt% In_2O_3 and 10 wt% SnO_2 with 99.999% purity, using an experimental

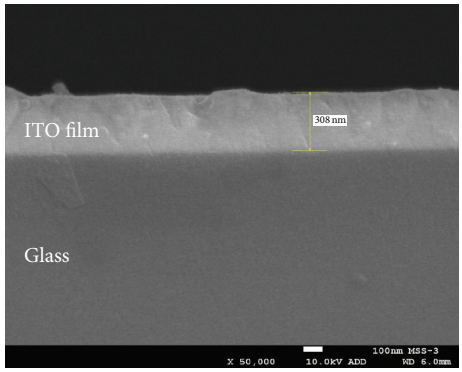

Figure 1: Cross-sectional SEM image of as-deposited ITO film on glass.

setup that has been used elsewhere [22–25]. Glass substrates were placed vertically in a suitable frame and moved in front of the target to deposit ITO at room temperature.

Highly pure argon and oxygen were introduced to a vacuum chamber using independent mass flow controllers after the vacuum chamber had been evacuated to a pressure of less than 1.0×10^{-5} torr. The final pressure thus reached was fixed at 1.1×10^{-3} torr. The applied sputtering power was 2.5 kW. All films were deposited at room temperature. The thickness of each deposited ITO film was approximately 300 nm (Figure 1). Following the deposition process, some of the samples were annealed at various temperatures (as-grown/100°C/200°C/300°C/400°C) for 30 min in air. The structural, optical, and electrical characteristics of the ITO coatings were analyzed as functions of the deposition and annealing parameters by X-ray diffraction (XRD), scanning electron microscopy (SEM), UV-VIS transmission spectroscopy, photoluminescence (PL) spectrophotometry, and the making of Hall effect measurements. Moreover, fabricate of a glass/Mo/CIGS/CdS/ZnO/ITO solar cell, and annealing at a best temperature for 30 min in air. *I-V* characteristics of CIGS solar cell can be obtained by using simulated standard test conditions of AM1.5.

3. Results and Discussion

3.1. XRD Measurements. Figure 2(a) presents XRD patterns of the ITO films that were deposited at room temperature using a fixed oxygen/argon ratio of 0.03 and then annealed at various temperatures (as-grown/100°C/200°C/300°C/400°C) for 30 min in air. The XRD measurements were made by scanning the diffraction angle from 20 to 65° at a grazing angle of incidence of 2°. The XRD patterns in Figure 2(a) reveal that the deposited and annealed ITO samples yielded many diffraction peaks at (211), (222), (400), (440), and (622), corresponding to various crystalline structures. As the substrate temperature is reduced, the mobility of the atoms and the particles that are deposited on the substrate falls. The probabilities of interaction are thereby also reduced. The polycrystalline films that were formed herein contained many structural defects and a nonstoichiometric composition. Postannealing can oxidize nonstoichiometric films, such as In_2O_{3-x} and SnO_{2-x} [26], and rearrange their atoms to produce stable polycrystalline films. In air, free oxygen may react with the stable polycrystalline films thus formed, improving their crystalline structures, as is revealed by the peak intensities from the annealed films herein. The deposited ITO films in this work have a cubic bixbyite structure of indium oxide with a strong preferential orientation. No evidence of a separate tin oxide phase was obtained herein. Samples that were deposited in pure argon exhibited no preferential crystalline orientation, whereas the XRD diffraction patterns of the ITO films that were deposited at high PO_2 (10% or more) exhibited a preferred [111] orientation, as revealed by the strong (222) peak, consistent with the literature [27]. The lattice distortion calculated with reference to the ideal lattice of In_2O_3 [28] was less than 0.8%.

Notably, all of the as-grown ITO thin films in this work exhibited the (222) preferred orientation. Figure 2(b) shows the XRD intensities of the (222) and (400) planes (I_{222} and I_{400}) and Figure 2(c) presents their total crystallinity, which was obtained by summing the intensities of the XRD peaks ($I_{222} + I_{400}$) and by calculating the ratio of the XRD peak intensities (I_{222}/I_{400}). As presented in Figures 2(b) and 2(c), the XRD patterns that were obtained following deposition with a fixed oxygen/argon ratio of 0.03 and annealing at various temperatures (as-grown/100°C/200°C/300°C/400°C) for 30 min in air have the interesting features; at a fixed oxygen/argon ratio (0.03), the XRD peak intensities of the (222) and (400) planes I_{200} and I_{400} and $I_{222} + I_{400}$ and the peak ratio I_{222}/I_{400} decreased stepwise as the annealing temperature increased (as-grown/100°C/200°C/300°C/400°C). The increase in the intensity ratio I_{222}/I_{400} with the substrate temperature and the increase upon postannealing treatment are strongly consistent with the literature [29]. Generally, the preferred (222) orientation of ITO thin films on glass substrates is strongly related to adatom mobility [30].

The samples herein exhibited (222)-orientated crystalline growth following annealing above 100°C, with extensive structural distortion (Figures 2(a)–2(c)). As the annealing temperature is increased, the lattices in the grains relaxed and some oxygen entered penetrated the grain boundaries [31].

3.2. Transmission Measurements. Figure 3(a) presents the total transmission spectra (400–1200 nm), and Figure 3(b) presents the visible (400–800 nm) and near-IR (800–1200 nm) transmission spectra of the ITO films that were deposited at room temperature using a fixed oxygen/argon ratio of 0.03 and then annealed at various temperatures (as-grown/100°C/200°C/300°C/400°C) in air. And Table 1 provided the transmission measurements data. Annealing (400°C) increased the average transmissions (400–1200 nm) of the ITO film by 16.36%. Figure 3(a) reveals that the fundamental absorption edge of the ITO film shifted to shorter wavelengths as the annealing temperature increased. Meng et al. reported [32] an accompanying increase in the carrier concentration, which is known as the Burstein-Moss shift. The Fermi level of a heavily doped n-type semiconductor is such that the bottom of the conduction band bottom is filled, causing the absorption edge to shift to higher energies with an increase in doping.

Table 1: Data concerning the ITO films annealing before and after annealing.

Samples	Parameters					
	Carrier concentration (cm^{-3})	Mobility (cm^2/Vs)	Resistivity (Ohm-cm)	Transmission (400–1200 nm) (%)	Transmission (400–800 nm) (%)	Transmission (800–1200 nm) (%)
As-grown	$-3.73E+20$	$2.29E+01$	$7.32E-04$	79.04	77.14	80.96
After annealing (100°C)	$-3.61E+20$	$2.38E+01$	$7.27E-04$	79.38	77.81	80.96
After annealing (200°C)	$-5.55E+20$	$2.26E+01$	$4.99E-04$	75.39	83.79	67.01
After annealing (300°C)	$-5.93E+20$	$2.48E+01$	$4.25E-04$	85.11	87.84	82.37
After annealing (400°C)	$-1.63E+20$	$2.71E+01$	$1.42E-03$	91.97	89.16	94.77

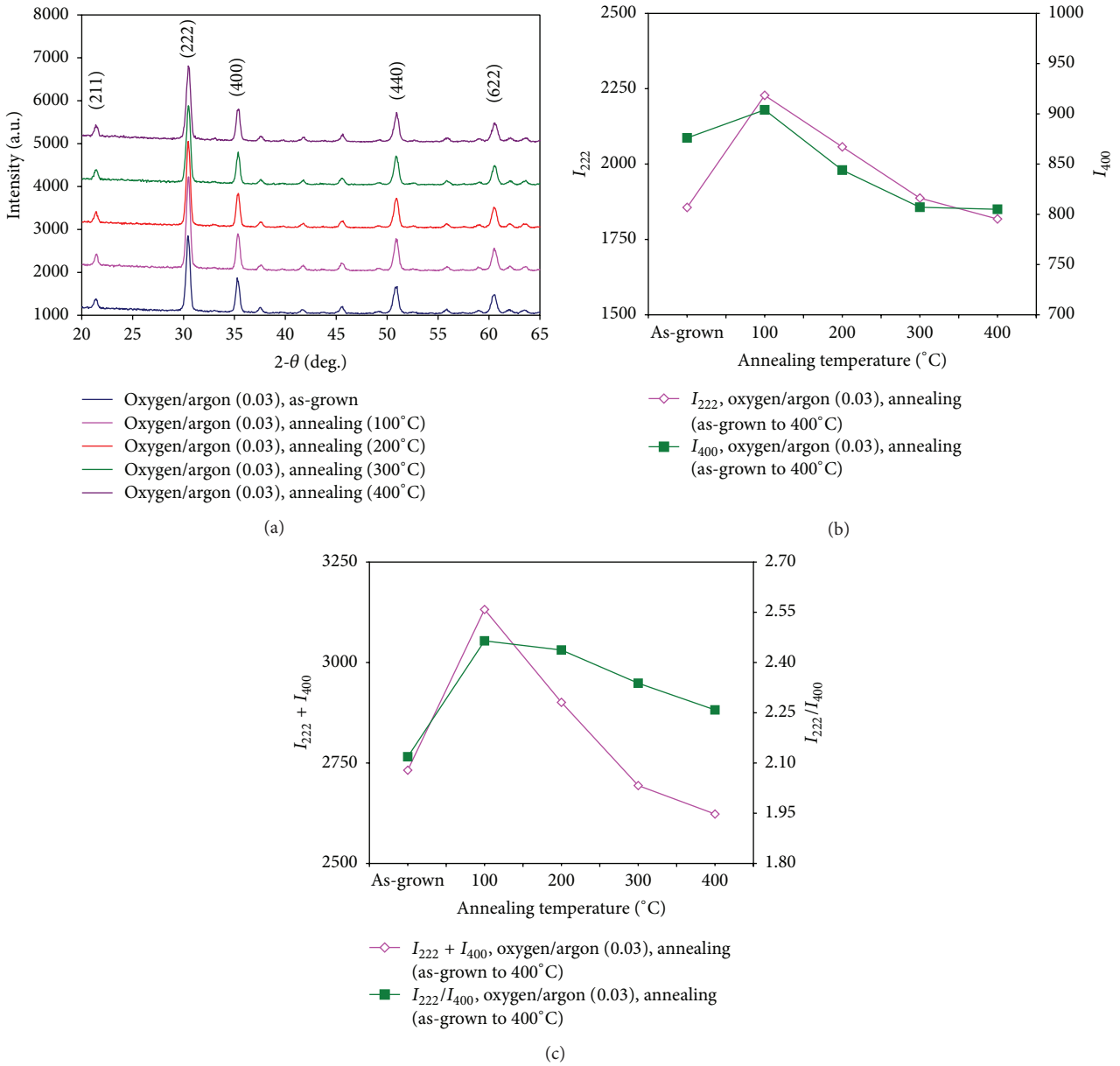

Figure 2: (a) XRD patterns of ITO thin films deposited using fixed oxygen/argon ratio (0.03) and annealed at various temperatures (as-grown/100°C/200°C/300°C/400°C), (b) XRD intensities of (222) and (400) planes (I_{222} and I_{400}), and (c) total crystallinity obtained by summing intensities of XRD peaks ($I_{222} + I_{400}$) and ratio of XRD peak intensities (I_{222}/I_{400}).

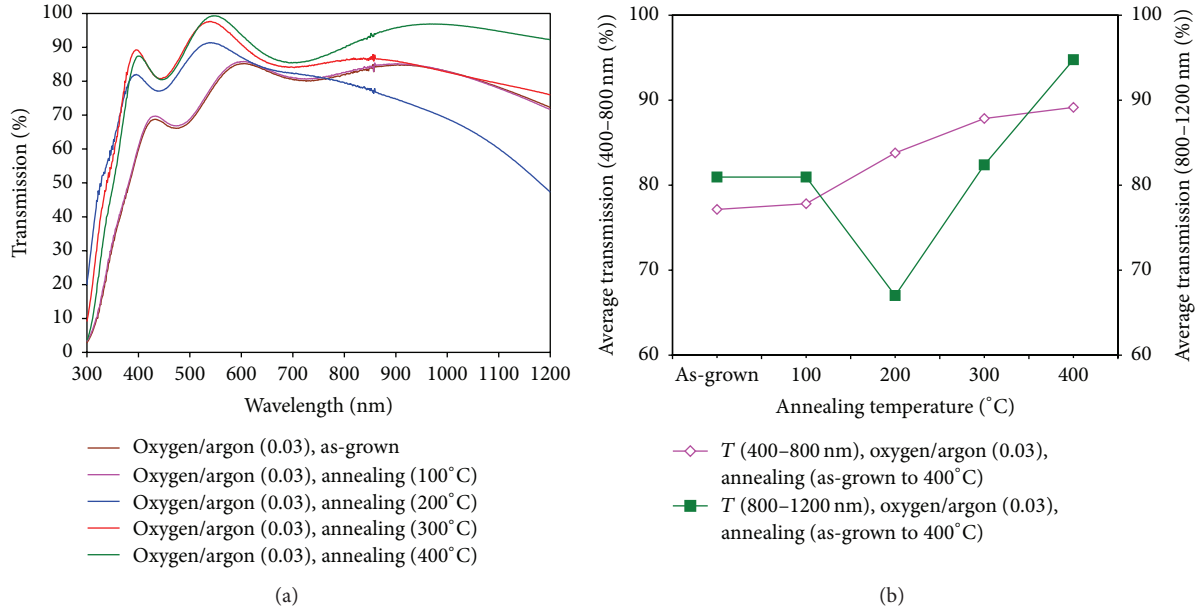

Figure 3: (a) Transmission spectra in visible and near-IR regions for ITO films deposited at room temperature at fixed oxygen/argon ratio (0.03) and annealed at various temperatures (as-grown/100°C/200°C/300°C/400°C) and (b) average visible-light (400–800 nm) and near-IR (800–1200 nm) transmissions of films deposited using a fixed oxygen/argon ratio of 0.03 and annealed at various temperatures (as-grown/100°C/200°C/300°C/400°C).

Table 1 and Figures 3(a) and 3(b) clearly reveal that the ITO films are deposited at room temperature with a fixed oxygen/argon ratio of 0.03; after that, the ITO films annealing at various temperatures (as-grown/100°C/200°C/300°C/400°C) improves their transmission of visible and near-IR lights. In the visible-light (400–800 nm) and near-IR (800–1200 nm) regions, the average transmissions of the as-grown ITO film that was deposited in an oxygen/argon ratio of 0.03 were approximately 77.1% and 80.9%, respectively; these values increased to more than 89.1% and 94.7% for the films that were annealed at 400°C in air. Annealing therefore improved the average transmissions of visible (400–800 nm) and near-IR (800–1200 nm) lights by 15.58% and 17.10%, respectively. The effects of annealing on crystallization reveal that the transmission of visible light through ITO films is closely related to their structure. The surface morphology of films also influences their transmission. The two scattering mechanisms in polycrystalline ITO films are ionized impurity scattering and grain boundary scattering; the dominant mechanism is the latter, as was discussed by Wu and Chiou [33]. As the sizes of the surface grain increase, the fewer grain boundaries scatter less light, increasing transmission in the visible region. Postannealing also favors oxidation of the ITO film compounds with a lower valence state [26]. These effects improve the transmission of visible light in the films. However, carrier absorption importantly affects the transmission of near-IR light through ITO films. The film that was annealed at 400°C in air exhibited the highest transmission. Therefore, most of the scattering of light in the films was Rayleigh scattering [34].

3.3. Electrical Measurements. The transmission of light in the near-IR light region (800–1200 nm) was related to resistivity, carrier concentration, and mobility, as presented in Figures 4(a)–4(c) and Table 1. In Figure 4(a), the high average transmission (800–1200 nm) and high resistivity of the film that was deposited at a fixed oxygen/argon ratio of 0.03 and annealed at 400°C are approximately 94.7% and $1.4E-03$ Ohm-cm, respectively, and the film that was annealed at 300°C had a lower resistivity of $4.2E-04$ Ohm-cm and an average transmission (800–1200 nm) of 87.8%. In Figure 4(b), the high average transmission (800–1200 nm) and low carrier concentration in the film that was deposited at a fixed oxygen/argon ratio of 0.03 and annealed at 400°C were approximately 94.7% and $-1.6E+20\ \text{cm}^{-3}$, respectively. The corresponding values for the film that was annealed at 300°C were 82.3% and $-5.9E+20\ \text{cm}^{-3}$. In Figure 4(c), the average transmission (800–1200 nm) and mobility for the film that was deposited at a fixed oxygen/argon ratio of 0.03 and annealed at 400°C are approximately 94.7% and $2.7E+01\ \text{cm}^2/\text{Vs}$, respectively, and those for the film that was annealed at 300°C are 82.3% and $2.4E+01\ \text{cm}^2/\text{Vs}$, respectively. According to Figures 4(b) and 4(c), the carrier concentration and mobility are strongly related to the structure of the film, a result which is consistent with the findings of Meng and dos Santos [35]. Some electrons in polycrystalline films are bound within a small volume of crystals grains in their nonuniform net structure. When such films become crystalline, these electrons are released from these bounded volumes, increasing the carrier concentration. We assert that close to the polycrystalline-crystalline transition point, the lattice

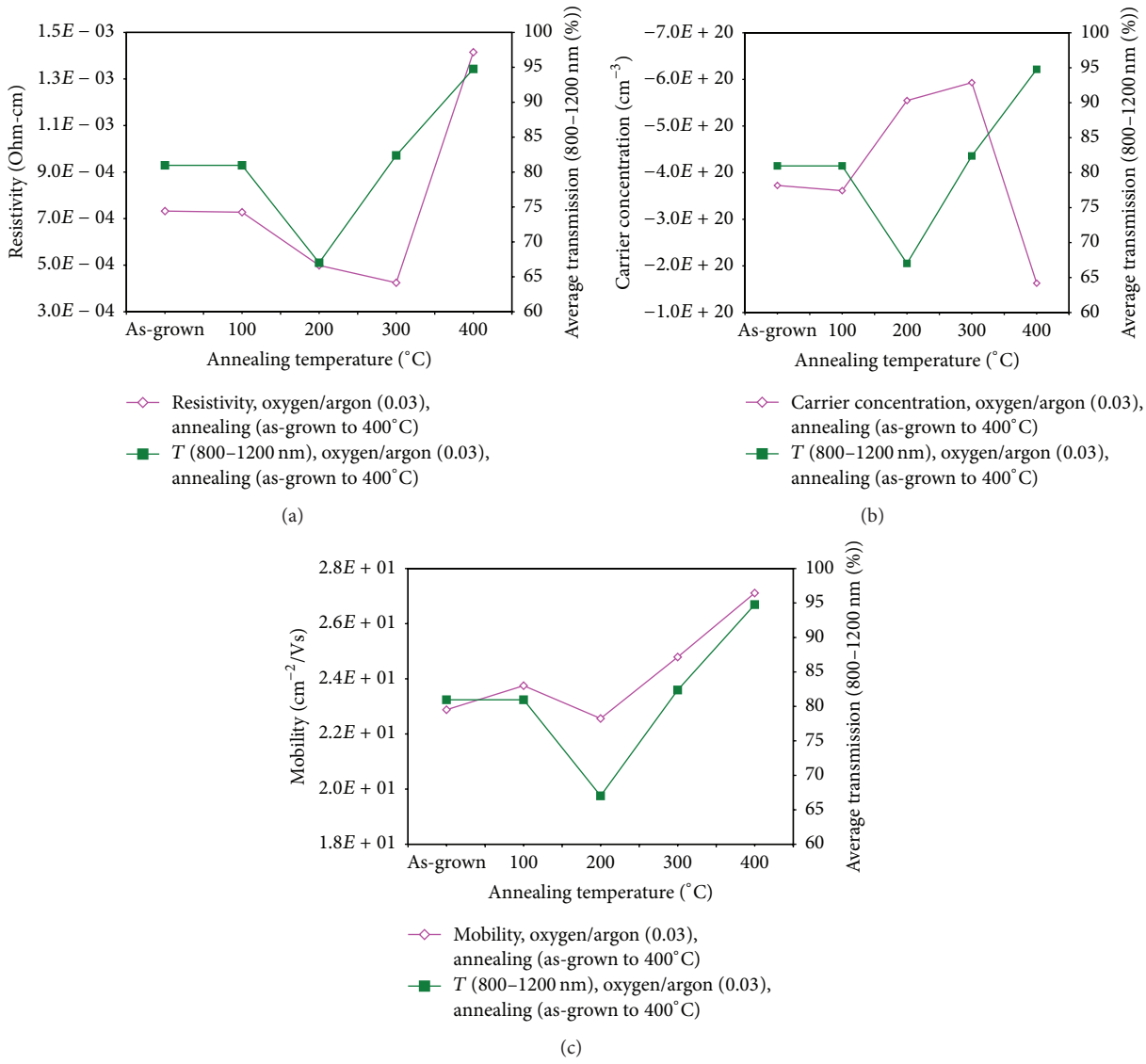

FIGURE 4: (a) Average transmission (800–1200 nm) and resistivity of films deposited at a fixed oxygen/argon ratio of 0.03 and annealed at various temperatures (as-grown/100°C/200°C/300°C/400°C), (b) average transmission (800–1200 nm) and carrier concentration of films deposited at a fixed oxygen/argon ratio of 0.03 and annealed at various temperatures (as-grown/100°C/200°C/300°C/400°C), and (c) average transmission (800–1200 nm) and mobility of films deposited at a fixed oxygen/argon ratio of 0.03 and annealed at various temperatures (as-grown/100°C/200°C/300°C/400°C).

transition strongly influences carrier mobility. Since indium in In_2O_3 has a valence of three, the presence of SnO_2 therein would result in n-doping of the lattice because the dopant would add electrons to the conduction band. In contrast, the presence of SnO would reduce the electron density in the conduction band. Some authors believe that, at low substrate temperature, SnO reduces carrier density and annealing transforms SnO into SnO_2, forming an n-type semiconductor with high carrier density and low resistivity [36–39]. According to Hu et al. [21], high-transmission films have a low carrier concentration, consistent by Hall effect measurements, as discussed below. In this work, ITO films were deposited at room temperature using a fixed oxygen/argon ratio of 0.03 and annealed at various temperatures in air such that the free oxygen in the air reacted with them. This reaction reduced the number of oxygen vacancies and the carrier concentration, increasing the resistivity of the films, which is strongly influenced by DC sputtering deposition using a fixed oxygen/argon ratio of 0.03 and the temperature of annealing. At a fixed oxygen/argon ratio, as the annealing temperature increased, the resistivity increased, the carrier concentration declined, and the transmission increased.

3.4. PL Measurements. PL measurements of the ITO films were made at room temperature. Figure 5 presents a typical PL spectrum of the ITO thin films that were deposited at a fixed oxygen/argon ratio of 0.03 and annealed at various temperatures (as-grown/100°C/200°C/300°C/400°C). Two bands

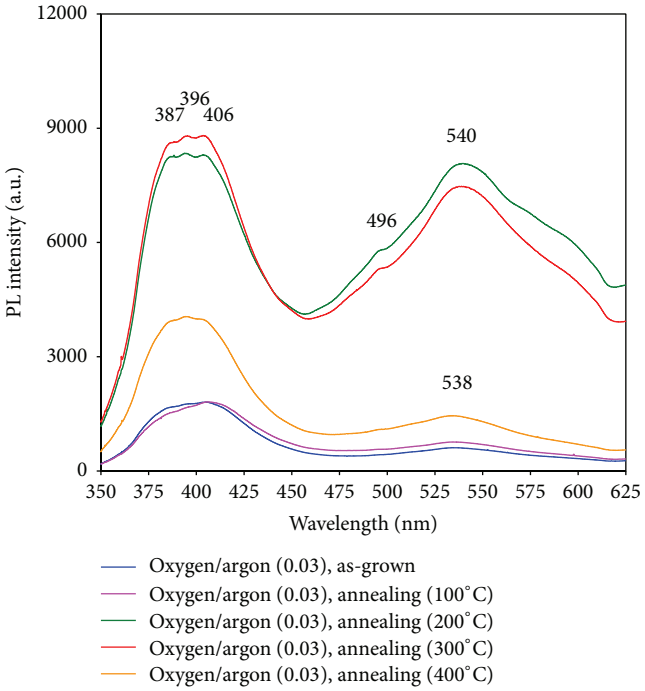

Figure 5: PL spectra of ITO thin films deposited using a fixed oxygen/argon ratio of 0.03 and annealed at various temperatures (as-grown/100°C/200°C/300°C/400°C).

Table 2: Data concerning the CIGS solar cell annealing before and after annealing.

Samples	Parameters				
	Area (cm^2)	Efficiency (%)	V_{oc} (V)	J_{sc} (mA/cm^2)	FF (%)
Before annealing	0.35	3.382	0.367	30.19	30.51
After annealing	0.35	4.016	0.368	31.89	34.20

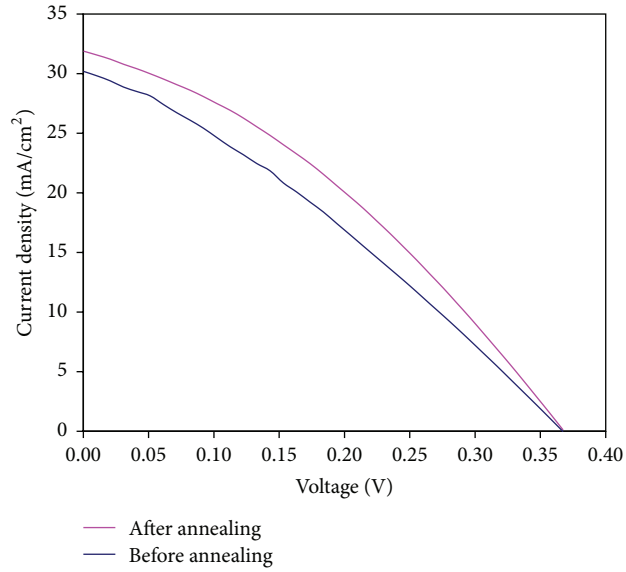

Figure 6: The illuminated *I-V* characteristics of CIGS solar cell annealing before and after annealing.

in the visible region are observed; these are more intense than the band excitation edge, indicating poor crystallinity of the ITO film. The less intense band is in the violet-blue region and includes three broad peaks at 387 nm (3.20 eV), 396 nm (3.13 eV), and 406 nm (3.05 eV). In each case, the peak at ~400 nm may be related to the emission of free excitons [40, 41], which are not trapped in defect centers. If the excitons are bound with the phonons, then many inflexions may appear in the broad emission band owing to the exciton-phonon interaction [42]. The second more intense band in the other part of the visible region (from blue to green) has a shoulder at 496 nm (2.50 eV) and a broad peak at 536–540 nm (2.30~2.31 eV). The broad peak at 536–540 nm may originate from strong photo emissions that are caused by some defects. Therefore, many defect levels may lie between the valence band and the conduction band, so most of the emitted photons are in the visible region.

3.5. Applications of CIGS Solar Cell. A glass/Mo/CIGS/CdS/ZnO/ITO solar cell was fabricated. This CIGS solar cell was annealed at 400°C for 30 min in air to improve its performance. *I-V* characteristics of CIGS solar cell can be obtained by using simulated standard test conditions of AM1.5. Table 2 presents data concerning the CIGS solar cell annealing before and after annealing. Figure 6 plots the illuminated *I-V* characteristics of the nonannealed and annealed solar cell. Annealing increased the efficiency of the CIGS solar cell by 18.75% (from 3.318% to 4.016%). The main improved parameters are open circuit voltage (V_{oc}), which is improved by 0.27% (from 0.367 to 0.368 V), current density (J_{sc}), which is improved by 5.63% (from 30.19 to 31.89%), and fill factor (FF), which is improved by 12.09% (from 30.51 to 34.20%). Therefore, the efficiency, which is the average transmission (400–1200 nm) of the ITO film, was improved by 16.36%. Additionally, annealing (400°C) improved the average transmissions of visible (400–800 nm) and near-IR (800–1200 nm) lights by the ITO films by 15.58% and 17.10%, respectively. Chen et al. [43] found that the transmission of short wavelengths ($\lambda < 800$ nm) is strongly affected by surface recombination, whereas that of long wavelengths ($\lambda > 850$ nm) is strongly influenced by bulk recombination. Liu et al. [44] found that the reflection of these wavelengths was related to surface recombination and bulk recombination, respectively. The solar cell absorbs light with wavelengths from 350 to 1200 nm, so increasing the transmission of light of these wavelengths can effectively increase the efficiency of solar cells [44–46]. Even if some points addressed on high-quality CIGS solar cells had been reported [47, 48], we would still like to verify them because our current study aims to enhance the methodology of research in this paper.

4. Conclusions

ITO thin films were grown on glass substrates by DC magnetron reactive sputtering at room temperature. An ITO sample with a highly crystalline structure was obtained by

deposition (at OR) using an oxygen/argon ratio of 0.03, followed by annealing at 400°C for 30 min. Annealing increased the average transmission (400–1200 nm) of the ITO film by 16.36% and the efficiency of a CIGS device that included such a film by 18.75%. These results are very encouraging for the future fabrication of CIGS solar cells with ITO films that are deposited using DC magnetron sputtering at room temperature and postdeposition annealing.

Conflict of Interests

The authors declare that there is no conflict of interests regarding the publication of this paper.

References

[1] K. L. Chopra, S. Major, and D. K. Pandya, "Transparent conductors—a status review," *Thin Solid Films*, vol. 102, no. 1, pp. 1–46, 1983.

[2] K. L. Chopra, P. D. Paulson, and V. Dutta, "Thin-film solar cells: an overview," *Progress in Photovoltaics: Research and Applications*, vol. 12, no. 2-3, pp. 69–92, 2004.

[3] T. M. Razykov, C. S. Ferekides, D. Morel, E. Stefanakos, H. S. Ullal, and H. M. Upadhyaya, "Solar photovoltaic electricity: current status and future prospects," *Solar Energy*, vol. 85, no. 8, pp. 1580–1608, 2011.

[4] P. Jackson, D. Hariskos, R. Wuerz et al., "Properties of $Cu(In,Ga)Se_2$ solar cells with new record efficiencies up to 21.7%," *Physica Status Solidi*, vol. 9, no. 1, pp. 28–31, 2015.

[5] Y. Yao, C. Jin, Z. Dong, Z. Sun, and S. M. Huang, "Improvement in performance of GaN-based light-emitting diodes with indium tin oxide based transparent ohmic contacts," *Displays*, vol. 28, no. 3, pp. 129–132, 2007.

[6] S. M. Huang, Y. Yao, C. Jin, Z. Sun, and Z. J. Dong, "Enhancement of the light output of GaN-based light-emitting diodes using surface-textured indium-tin-oxide transparent ohmic contacts," *Displays*, vol. 29, no. 3, pp. 254–259, 2008.

[7] Y.-C. Park, Y.-S. Kim, H.-K. Seo, S. G. Ansari, and H.-S. Shin, "ITO thin films deposited at different oxygen flow rates on Si(100) using the PEMOCVD method," *Surface and Coatings Technology*, vol. 161, no. 1, pp. 62–69, 2002.

[8] A. Suzuki, T. Matsushita, T. Aoki, A. Mori, and M. Okuda, "Highly conducting transparent indium tin oxide films prepared by pulsed laser deposition," *Thin Solid Films*, vol. 411, no. 1, pp. 23–27, 2002.

[9] S. Seki, Y. Sawada, and T. Nishide, "Indium-tin-oxide thin films prepared by dip-coating of indium diacetate monohydroxide and tin dichloride," *Thin Solid Films*, vol. 388, no. 1-2, pp. 22–26, 2001.

[10] D. Kim, Y. Han, J.-S. Cho, and S.-K. Koh, "Low temperature deposition of ITO thin films by ion beam sputtering," *Thin Solid Films*, vol. 377-378, pp. 81–86, 2000.

[11] F. El Akkad, A. Punnoose, and J. Prabu, "Properties of ITO films prepared by rf magnetron sputtering," *Applied Physics A: Materials Science & Processing*, vol. 71, no. 2, pp. 157–160, 2000.

[12] A. Luis, C. N. de Carvalho, G. Lavareda, A. Amaral, P. Brogueira, and M. H. Godinho, "ITO coated flexible transparent substrates for liquid crystal based devices," *Vacuum*, vol. 64, no. 3-4, pp. 475–479, 2002.

[13] F. L. Wong, M. K. Fung, S. W. Tong, C. S. Lee, and S. T. Lee, "Flexible organic light-emitting device based on magnetron sputtered indium-tin-oxide on plastic substrate," *Thin Solid Films*, vol. 466, no. 1-2, pp. 225–230, 2004.

[14] D. Kim and S. Kim, "AFM observation of ITO thin films deposited on polycarbonate substrates by sputter type negative metal ion source," *Surface and Coatings Technology*, vol. 176, no. 1, pp. 23–29, 2003.

[15] H.-Y. Yeom, N. Popovich, E. Chason, and D. C. Paine, "A study of the effect of process oxygen on stress evolution in d.c. magnetron-deposited tin-doped indium oxide," *Thin Solid Films*, vol. 411, no. 1, pp. 17–22, 2002.

[16] Y.-S. Kim, Y.-C. Park, S. G. Ansari, J.-Y. Lee, B.-S. Lee, and H.-S. Shin, "Influence of O_2 admixture and sputtering pressure on the properties of ITO thin films deposited on PET substrate using RF reactive magnetron sputtering," *Surface and Coatings Technology*, vol. 173, no. 2-3, pp. 299–308, 2003.

[17] T. Seino, T. Sato, and M. Kamei, "650 mm × 830 mm area sputtering deposition using a separated magnet system," *Vacuum*, vol. 59, no. 2-3, pp. 431–436, 2000.

[18] S. J. Nadel, P. Greene, J. Rietzel, and J. Strümpfel, "Equipment, materials and processes: a review of high rate sputtering technology for glass coating," *Thin Solid Films*, vol. 442, no. 1-2, pp. 11–14, 2003.

[19] H. Morikawa and M. Fujita, "Crystallization and electrical property change on the annealing of amorphous indium-oxide and indium-tin-oxide thin films," *Thin Solid Films*, vol. 359, no. 1, pp. 61–67, 2000.

[20] Y. S. Jung, "A spectroscopic ellipsometry study on the variation of the optical constants of tin-doped indium oxide thin films during crystallization," *Solid State Communications*, vol. 129, no. 8, pp. 491–495, 2004.

[21] Y. Hu, X. Diao, C. Wang, W. Hao, and T. Wang, "Effects of heat treatment on properties of ITO films prepared by rf magnetron sputtering," *Vacuum*, vol. 75, no. 2, pp. 183–188, 2004.

[22] J. B. Almeida, "Design of magnetrons for dc sputtering," *Vacuum*, vol. 39, no. 7-8, pp. 717–721, 1989.

[23] F. Kurdesau, G. Khripunov, A. F. da Cunha, M. Kaelin, and A. N. Tiwari, "Comparative study of ITO layers deposited by DC and RF magnetron sputtering at room temperature," *Journal of Non-Crystalline Solids*, vol. 352, no. 9–20, pp. 1466–1470, 2006.

[24] H.-N. Cui, V. Teixeira, L.-J. Meng, R. Martins, and E. Fortunato, "Influence of oxygen/argon pressure ratio on the morphology, optical and electrical properties of ITO thin films deposited at room temperature," *Vacuum*, vol. 82, no. 12, pp. 1507–1511, 2008.

[25] K. J. Kumar, N. R. C. Raju, and A. Subrahmanyam, "Thickness dependent physical and photocatalytic properties of ITO thin films prepared by reactive DC magnetron sputtering," *Applied Surface Science*, vol. 257, no. 7, pp. 3075–3080, 2011.

[26] I. Hamberg and C. G. Granqvist, "Evaporated Sn-doped In_2O_3 films: basic optical properties and applications to energy-efficient windows," *Journal of Applied Physics*, vol. 60, no. 11, pp. R123–R160, 1986.

[27] S.-I. Jun, T. E. McKnight, M. L. Simpson, and P. D. Rack, "A statistical parameter study of indium tin oxide thin films deposited by radio-frequency sputtering," *Thin Solid Films*, vol. 476, no. 1, pp. 59–64, 2005.

[28] Powder Diffraction File, Joint Committee on Powder Diffraction Standards—International Centre for Diffraction Data, Newtown Square, Pa, USA, Card 06-0416, 1981.

[29] L.-J. Meng and M. P. dos Santos, "Properties of indium tin oxide films prepared by rf reactive magnetron sputtering at different substrate temperature," *Thin Solid Films*, vol. 322, no. 1-2, pp. 56–62, 1998.

[30] H. Ma, J.-S. Cho, and C.-H. Park, "A study of indium tin oxide thin film deposited at low temperature using facing target sputtering system," *Surface and Coatings Technology*, vol. 153, no. 2-3, pp. 131–137, 2002.

[31] C. Guillén and J. Herrero, "Influence of oxygen in the deposition and annealing atmosphere on the characteristics of ITO thin films prepared by sputtering at room temperature," *Vacuum*, vol. 80, no. 6, pp. 615–620, 2006.

[32] L.-J. Meng, A. Maçarico, and R. Martins, "Study of annealed indium tin oxide films prepared by rf reactive magnetron sputtering," *Vacuum*, vol. 46, no. 7, pp. 673–680, 1995.

[33] W.-F. Wu and B.-S. Chiou, "Effect of annealing on electrical and optical properties of RF magnetron sputtered indium tin oxide films," *Applied Surface Science*, vol. 68, no. 4, pp. 497–504, 1993.

[34] I. Fanderlik, *Optical Properties of Glass*, Elsevier, Amsterdam, The Netherlands, 1983.

[35] L.-J. Meng and M. P. dos Santos, "Structure effect on electrical properties of ITO films prepared by RF reactive magnetron sputtering," *Thin Solid Films*, vol. 289, no. 1-2, pp. 65–69, 1996.

[36] G. Frank and H. Köstlin, "Electrical properties and defect model of tin-doped indium oxide layers," *Applied Physics A*, vol. 27, no. 4, pp. 197–206, 1982.

[37] C. H. L. Weijtens, "Influence of the deposition and anneal temperature on the electrical properties of indium tin oxide," *Journal of the Electrochemical Society*, vol. 138, no. 11, pp. 3432–3434, 1991.

[38] S. Bhagwat and R. P. Howson, "Use of the magnetron-sputtering technique for the control of the properties of indium tin oxide thin films," *Surface and Coatings Technology*, vol. 111, no. 2-3, pp. 163–171, 1999.

[39] Y. Shigesato and D. C. Paine, "Study of the effect of Sn doping on the electronic transport properties of thin film indium oxide," *Applied Physics Letters*, vol. 62, no. 11, pp. 1268–1270, 1993.

[40] S. Kundu and P. K. Biswas, "Synthesis and photoluminescence property of nanostructured sol-gel indium tin oxide film on glass," *Chemical Physics Letters*, vol. 414, no. 1–3, pp. 107–110, 2005.

[41] A. El Hichou, A. Kachouane, J. L. Bubendorff et al., "Effect of substrate temperature on electrical, structural, optical and cathodoluminescent properties of In_2O_3-Sn thin films prepared by spray pyrolysis," *Thin Solid Films*, vol. 458, no. 1-2, pp. 263–268, 2004.

[42] S.-F. Ren, Z.-Q. Gu, and D. Lu, "Quantum confinement of phonon modes in GaAs quantum dots," *Solid State Communications*, vol. 113, no. 5, pp. 273–277, 2000.

[43] Z. Chen, A. Rohatgi, R. O. Bell, and J. P. Kalejs, "Defect passivation in multicrystalline-Si materials by plasma-enhanced chemical vapor deposition of SiO_2/SiN coatings," *Applied Physics Letters*, vol. 65, no. 16, pp. 2078–2080, 1994.

[44] C. P. Liu, M. W. Chang, and C. L. Chuang, "Effect of rapid thermal oxidation on structure and photoelectronic properties of silicon oxide in monocrystalline silicon solar cells," *Current Applied Physics*, vol. 14, no. 5, pp. 653–658, 2014.

[45] D.-Y. Lee, H.-H. Lee, J. Y. Ahn et al., "A new back surface passivation stack for thin crystalline silicon solar cells with screen-printed back contacts," *Solar Energy Materials & Solar Cells*, vol. 95, no. 1, pp. 26–29, 2011.

[46] P. Panek, K. Drabczyk, A. Focsa, and A. Slaoui, "A comparative study of SiO_2 deposited by PECVD and thermal method as passivation for multicrystalline silicon solar cells," *Materials Science and Engineering B*, vol. 165, no. 1-2, pp. 64–66, 2009.

[47] K. Sharma, B. L. Williams, A. Mittal et al., "Expanding thermal plasma chemical vapour deposition of ZnO:Al layers for cigs solar cells," *International Journal of Photoenergy*, vol. 2014, Article ID 253140, 9 pages, 2014.

[48] S. Kijima and T. Nakada, "High-temperature degradation mechanism of Cu(In,Ga)Se_2-based thin film solar cells," *Applied Physics Express*, vol. 1, no. 7, Article ID 075002, 2008.